Amorphous Alumina Coatings: Processing, Structure and Remarkable Barrier Properties

Diane Samélor[1], Ana-Maria Lazar[1], Maëlenn Aufray[1], Claire Tendero[1], Loïc Lacroix[2], Jean-Denis Béguin[2], Brigitte Caussat[3], Hugues Vergnes[3], Joël Alexis[2], Dominique Poquillon[1], Nadine Pébère[1], Alain Gleizes[1], and Constantin Vahlas[1,*]

[1] *University of Toulouse, CIRIMAT/INP T, 4 allée Emile Monso BP 44362, 31030 Toulouse cedex 4, France*
[2] *University of Toulouse, LGP-ENIT/INP T, 47 avenue d'Azereix BP 1329, 65016 Tarbes, France*
[3] *University of Toulouse, LGC/INP T, 4 allée Emile Monso BP 84234, 31432 Toulouse cedex 4, France*

Amorphous aluminium oxide coatings were processed by metalorganic chemical vapour deposition (MOCVD); their structural characteristics were determined as a function of the processing conditions, the process was modelled considering appropriate chemical kinetic schemes, and the properties of the obtained material were investigated and were correlated with the nanostructure of the coatings. With increasing processing temperature in the range 350 °C–700 °C, subatmospheric MOCVD of alumina from aluminium tri-isopropoxide (ATI) sequentially yields partially hydroxylated amorphous aluminium oxides, amorphous Al_2O_3 (415 °C–650 °C) and nanostructured γ-Al_2O_3 films. A numerical model for the process allowed reproducing the non uniformity of deposition rate along the substrate zone due to the depletion of ATI. The hardness of the coatings prepared at 350 °C, 480 °C and 700 °C is 6 GPa, 11 GPa and 1 GPa, respectively. Scratch tests on films grown on TA6V titanium alloy reveal adhesive and cohesive failures for the amorphous and nanocrystalline ones, respectively. Alumina coating processed at 480 °C on TA6V yielded zero weight gain after oxidation at 600 °C in lab air. The surface of such low temperature processed amorphous films is hydrophobic (water contact angle 106 degrees), while the high temperature processed nanocrystalline films are hydrophilic (48 degrees at a deposition temperature of 700 °C). It is concluded that amorphous Al_2O_3 coatings can be used as oxidation and corrosion barriers at ambient or moderate temperature. Nanostructured with Pt or Ag nanoparticles, they can also provide anti-fouling or catalytic surfaces.

Keywords: MOCVD, Amorphous Alumina, Process Modeling, Mechanical Properties, Oxidation Resistance, Corrosion Resistance, Wetting.

1. INTRODUCTION

Due to its numerous allotropic modifications and to the subsequent large spectrum of structure-properties relationships, aluminium oxides in the form of films and coatings are of major technological interest for a wide panel of applications: optics and microelectronics components, wear resistance, catalyst support, protection against corrosion and high temperature oxidation. Metal Organic Chemical Vapor Deposition (MOCVD) is a potentially attractive technique for the processing of such coatings, especially on complex-in-shape, temperature sensitive parts. In this frame, processing-structure-properties relationships were established and the feasibility of such a process was proven at laboratory scale in a series of papers the authors' groups published in the last years.[1–6] The objective of this work is to resume these reports and to enrich them with original results, namely on the surface wetting of the different aluminium oxides and their performance as moderate temperature oxidation barriers. In that which follows, the microstructural characteristics of the coatings will be presented first, as a function of the processing conditions. Then, results on the modeling of the MOCVD process will be presented, followed by information on the performance of the coatings in terms of oxidation and corrosion resistance, wetting, electrochemical and mechanical behavior, prior providing concluding remarks.

*Author to whom correspondence should be addressed.

Table I. Processing conditions for the kinetic modeling. Total pressure 5 Torr, deposition temperature 480 °C and total flow rate 653 sccm in all runs.

Sample	T_{ATI} [°C]	Q_{ATI} [sccm]	Deposition rate [A/min]
E1	100	1.54	80–220
E2	110	3.40	293–651
E3	90	0.70	43–100
E4	80	0.31	18–53

2. EXPERIMENTAL DETAILS

Alumina coatings were prepared from a MOCVD process in a horizontal hot-wall reactor with an internal diameter of 26 mm. Deposition was investigated from Aluminium Tri Isopropoxide (ATI) as a precursor, at a low pressure of 5 Torr, in a temperature range varying from 350 °C to 700 °C and using nitrogen as carrier an dilution gas. The aluminium oxide films were deposited on TA6V, polished down to 4000 grade with SiC paper, and silicon substrates for the study of the films properties and the determination of the apparent kinetic law, respectively. The characteristics of the obtained films were previously reviewed and it was mentioned that composition, microstructure and crystallinity of the films can be adjusted by varying the processing conditions.[2] The processing conditions are detailed in Tables I and II. Films thickness for the properties tests are between 0.4 and 1.5 μm.

High temperature oxidation tests were conducted at 600 °C in a tube furnace under laboratory air. Samples were ultrasonically cleaned in acetone and ethanol and finally dried. Before the tests, the surface area of each sample was determined. Samples were introduced in the hot furnace; they were weighted before, during and after the oxidation tests using a Sarturius balance ($\pm$10 μg). Comparison with oxidation data from thermogravimetric experiments using a Setaram TAG24S instrument[15] revealed comparable oxidation kinetics. It is concluded that the adopted protocol consisting in periodically removing the samples from the furnace to weight them does not significantly modify the oxidation kinetics.

The contact angles were measured using a Digidrop Contact Angle Meter from GBX Scientific Instruments at room temperature. A known volume (3–5 μL) of ultrapure water (resistivity > 18 M Ohm) was deposited on the surface of the sample and then the static contact angle (θ) was measured after few seconds of stabilization of the interfacial forces. In order to assess the homogeneity of the surface properties, 12 measurements were performed on 6 drops deposited at different locations on the samples and the average contact angle was calculated.

Table II. Processing conditions for the properties tests. Total pressure 5 Torr and total flow rate 653 sccm in all runs.

Sample	T_{ATI} [°C]	Q_{ATI} [sccm]	Composition
A350			Amorphous AlO(OH)
B480	100	1.54	Amorphous Al_2O_3
C700			Nanocrystalline Al_2O_3

The samples were characterized by voltammetry (anodic and cathodic polarization curves). A three-electrode cell was used for the experiments: the coated Ti6242 coupons as working electrode, a saturated calomel reference electrode (SCE) and a platinum grid as auxiliary electrode. Experiments were performed in a 0.1 M NaCl solution at room temperature without stirring. The polarization curves were obtained after 1 h of immersion at the corrosion potential from cathodic to anodic potentials. The potential sweep rate was fixed at 0.277 $mV \cdot s^{-1}$.

The mechanical properties of the alumina coatings were studied by using a nanoindentor XP from MTS with a Dynamic Contact Module (DCM). This study consisted of a matrix of 20 measurements in the Continuous Stiffness mode, carried out with a Berkovitch indenter. These measurements were realized for each coating. A maximum in-depth displacement of 300 nm was fixed. The indent matrix was realized with a ten-micron step between each measurement to avoid work hardening. The Young's modulus of the coatings was calculated with the Eq. (1),[18]

$$S = \frac{dP}{dH} = \frac{2}{\sqrt{\pi}} E_r \sqrt{A(h_c)} \tag{1}$$

with S the contact stiffness (slope of the discharge curve at the highest load), P the applied load, H the indentation depth, $A(h_c)$ the contact area as a function of the indentation depth, E_r the effective Young's modulus of the system calculated with the Eq. (2),

$$\frac{1}{E_r} = \frac{1-v_i^2}{E_i} + \frac{1-v_s^2}{E_s} \tag{2}$$

with E_i and E_s the Young's moduli of the indentor and the sample respectively, ν_i and ν_s the Poisson's ratios of the indentor and the sample respectively.

3. RESULTS AND DISCUSSION

3.1. Process Modeling

3D modeling of the process was performed ultimately aiming at better understanding of the involved complex physical and chemical phenomena, at optimizing deposition conditions regarding film thickness, at designing more convenient reactor geometries in order to fulfil industrial specifications and to coat 3D massive pieces. Initiation of this task was detailed in Ref. [3]; main assumptions and results are resumed in the present work.

The bottleneck in the modeling of MOCVD of alumina from ATI is the scarcity of the insight in the chemical mechanisms and the kinetic data. This is generally true for

MOCVD processes for which the precursor molecules and then the involved chemical homogeneous and heterogeneous mechanisms are complex. There are some reports[8–14] dealing such mechanisms controlling the processing of aluminium oxide coatings from ATI, but they do not agree together. This discrepancy can be attributed to the different ranges of operating conditions investigated by the authors (temperature and pressure varying from 220 °C to 1080 °C, and from 3 Torr to 200 Torr, respectively), leading to different homogeneous and heterogeneous chemical reactions prevailing in each case. As no consensus and no consolidated chemical paths exist for the present operating range, a particular mechanism was adopted, based on factual elements. Sovar et al.[1] demonstrated that ATI keeps its tetrameric structure in the vapour phase; so this molecule was used as starting point. Since water and propylene were found as by-products of the deposition,[9] the following apparent chemical reaction was used:

$$[Al(OC_3H_7)_3]_{4(g)} \rightarrow 2Al_2O_{3(s)} + 12C_3H_{6(g)} + 6H_2O_{(g)} \quad \text{(R1)}$$

This reaction represents the whole homogeneous and heterogeneous chemical reactions involved. Following Hofman et al.[9] the alumina deposition rate R_{Di} (kg/m^2/s) is represented by the classical following apparent kinetic law:

$$R_{Di} = k_0 \exp(-Ea/RT)[ATI]^n \quad (3)$$

The kinetic parameters k_0, Ea and n were determined by using plug flow reactor assumption and by fitting calculated deposition rates with experimental ones for runs E1 to E3 (see Ref. [3] for more details). Then, the obtained kinetic parameters ($k_0 = 1.5\ 10^6$ kg · m$^{2.5}$/(mol$^{1.5}$s), Ea = 78 kJ/mol, $n = 1.5$) were implemented in a commercial CFD code Fluent from the Ansys Suite.[14] This software uses a Reynolds Average Navier-Stokes solver to determine the temperature, pressure, gas velocity and concentration profiles and also the deposition rate distribution on all solid surfaces of the reactor. Figure 1 compares experimental and simulated deposition rates along the reactor axis for runs E4 (not used for the fitting) and E3. A relatively good agreement is observed which allows validating the kinetic model for the range of operating conditions considered. Such fitting will be improved from the input of complementary experimental data. This approach could be generalized to other MOCVD processes.

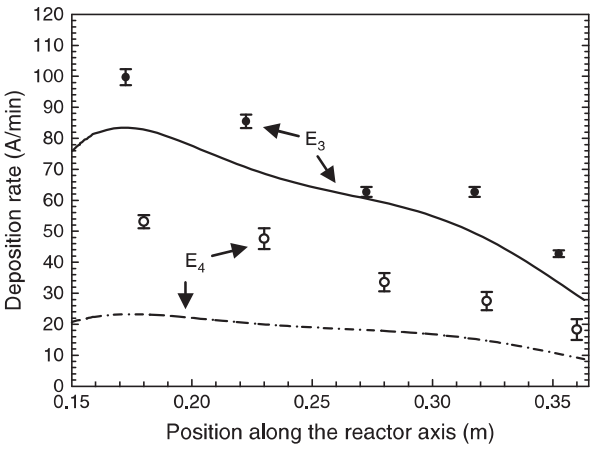

Fig. 1. Comparison between the experimental (circle) and the calculated (line) deposition rates along the reactor axis for runs E3 and E4.

3.2. Oxidation

Figure 2 compares oxidation kinetics of all the samples tested. NMG of reference sample corresponds to an oxidation kinetics rate of 4.6 10^{-8} mg$^2 \cdot$s$^{-1} \cdot$cm^{-4}. This value is in good agreement with the data available in literature for pure titanium[16, 17] and Ti-4.02 wt% Al.[7] All coatings allow for a significant decrease of the oxidation kinetics rate, the strongest decrease corresponding to the one processed at 480 °C. SEM observation of sample B480-2 reveal than oxidation may be exclusively due to coating cracks, located at the corners, near the edges of the samples. It is concluded that the non-crystalline stoechiometric aluminium oxide deposited at 480 °C offers interesting barrier properties and seems to reduce oxidation kinetics and diffusion of oxygen in TA6V. These results should be confirmed by processing uncracked coatings and by carrying out longer tests.

3.3. Wettability

Contact angle of water drops on samples A350 B480 and C700 are detailed in Table III. The results show that the contact angles increase with the deposition temperature: the amorphous surfaces, Al_2O_3 and AlO(OH), are hydrophobic and the crystalline surface is hydrophilic.

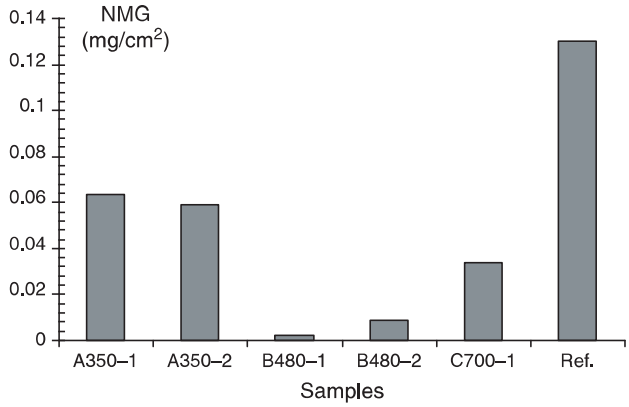

Fig. 2. Net Mass Gain (NMG) after 100 h at 600 °C under laboratory air. Ref sample stands for uncoated TA6V used as reference.

Table III. Wetting properties of the coatings tested with ultra-pure water.

Sample code	Contact angles	Surface behavior
A350	103 ± 1	Hydrophobic
B480	106 ± 2	Hydrophobic
C700	48 ± 3	Hydrophilic

3.4. Polarization Curves

The polarization curves obtained for the three different films deposited on TA6V are presented in Figure 3. The values of the corrosion potential are approximately the same independently of the coating. For the three samples, the anodic current density progressively increases as the potential increases. Sample B480 presents the lowest cathodic and anodic current densities. Thus, amorphous Al_2O_3 insulating coatings allow an improvement of the corrosion resistance. Amorphous AlO(OH) coatings (A350) provide limited corrosion protection attributed to their lamellar nanostructure and to the presence of reactive hydroxo groups. The crystallized alumina containing coatings (C700) provide intermediate corrosion protection probably due to the presence of grain boundaries which favor electrolyte penetration through the film.

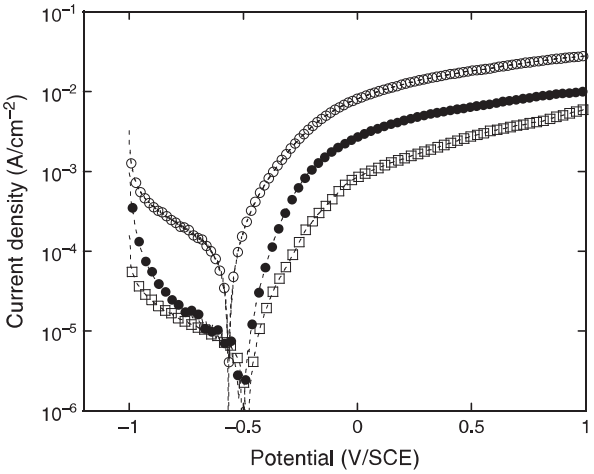

Fig. 3. Polarization curves for the three different aluminium oxide coatings plotted from cathodic to anodic potentials in 0.1 M NaCl solution (○) A350, (□) B480 and (•) C700.

Table IV. Mechanical properties of the CVD alumina coatings.

Sample code	Young's modulus (GPa)	Hardness (GPa)
A350	90	6
B480	155	11
C700	10	1

3.5. Mechanical Properties

The Young's modulus and hardness values of the CVD alumina coatings on TA6V alloy were obtained by nanoindentation for the three different deposition temperatures. Table IV presents the mechanical properties of the coatings.

Both amorphous coatings have higher Young's modulus values (90 GPa and 155 GPa for the samples A350 and B480 respectively) than the sample C700 (10 GPa). The same trend can be observed for the hardness values.

4. CONCLUSIONS

3D modeling of the MOCVD of aluminium oxide from ATI presents potential for the optimization of process in the perspective to treat complex shaped pieces. Such coatings, processed in the range 420 °C–650 °C are composed of stoechiometric, amorphous alumina. They present attractive barrier properties, as is illustrated by their electrochemical behaviour and by dedicated tests. Their surface and mechanical properties can be monitored as a function of the processing conditions.

The as established processing—structure—properties relation paves the way to engineer MOCVD aluminium oxide complex coatings which meet specifications such as oxidation and corrosion barrier.

Acknowledgments: The authors would like to thank the tinancial support of the Institut National Polytechnique de Toulouse through a Bonus Qualité Recherche grant.

References and Notes

1. M. M. Sovar, D. Samélor, A. N. Gleizes, and C. Vahlas, *Surf. Coat. Techn.* 201 9159 (**2007**).
2. A. Gleizes, C. Vahlas, M. M. Sovar, D. Samélor, and M. C. Lafont, *Chem. Vap. Dep.* 13, 23 (**2007**).
3. H. Vergnes, D. Samelor, A. Gleizes, C. Vahlas, and B. Caussat, *Chem. Vap. Dep.*, to be published.
4. J. D. Béguin, D. Samélor, C. Vahlas, A. Gleizes, J. A. Peti, and B. Sheldon, *Mat. Sci. Forum* 595–598, 719 (**2008**).
5. G. Boisier, M. Raciulete, D. Samélor, N. Pébère, A. N. Gleizes, and C. Vahlas, *Electrochem. Sol. State Lett.* 11, C55 (**2008**).
6. Y. Balcaen, N. Radutoiu, J. Alexis, J.-D. Beguin, L. Lacroix, D. Samélor, and C. Vahlas, *Surf. Coat. Techn.*, submitted.
7. A. M. Chaze and C. Coddet, *J. Less Common Met.* 157, 55 (**1990**).
8. M. Kawase, Y. Ikuta, T. Tago, T. Masuda, and K. Hashimoto, *Schem. Eng. Sci.* 49, 4861 (**1994**).
9. R. Hofman, R. W. J. Morssinkhof, T. Fransen, J. G. F. Westheim, and P. J. Gellings, *Mat. Manuf. Proc.* 8, 315 (**1993**).
10. S. Blittersdorf, N. Bahlawane, K. Kohse-Höinghaus, B. Atakan, and J. Müller, *Chem. Vap. Dep.* 9, 194 (**2003**).
11. J. Saraie, K. Ono, and S. Takeuchi, *J. Electrochem. Soc.* 136, 3139 (**1989**).
12. M. Kawase and K. Miura, *Thin Solid Films* 498, 25 (**2006**).

13. D. H. Lee, D. J. Choi, and S. H. Hyun, *J. Mater. Sci. Lett.* 15, 96 **(1996)**.
14. Fluent is a product of Ansys Inc., Canonsburg, PA, USA, (www.fluent.com).
15. D. Samélor, M. Aufray, L. Lacroix, Baelcan, J. Alexis, H. Vergnes, D. Poquillon, J-D. Beguin, N. Pébère, S. Marcelin, B. Caussat, and C. Vahlas, *CIMTEC 2010-12th International Conference on Modern Materials and Technologies*, Montecatini Terme, Tuscany, Italy **(2010)**.
16. P. Kofstad, K. Hauffe, and H. Kjollesdal, *Acta Chem. Scand.* 12, 259 **(1958)**.
17. P. Kofstad, High Temperature Oxidation of Metals, Wiley, NY **(1966)**.
18. W. C. Oliver and G. M. Pharr, *J. Mater. Res.* 7, 1564 **(1992)**.